

Nonunique Structure of Metastable $(\text{GaSb})_{1-x}(\text{Ge}_2)_x$ Alloys

E. A. Stern, F. Ellis,^(a) and K. Kim

Department of Physics, University of Washington, Seattle, Washington 98195

and

L. Romano, S. I. Shah, and J. E. Greene

*Department of Metallurgy, Coordinated Science Laboratory, Materials Research Laboratory,
University of Illinois, Urbana, Illinois 61801*

(Received 3 December 1984)

A combination of x-ray diffraction and extended x-ray-absorption fine-structure analyses were used to show that an order-disorder structural transition from zinc blende to diamond occurs in metastable $(\text{GaSb})_{1-x}(\text{Ge}_2)_x$ alloys at a critical composition x_c even though the short-range order remains perfect throughout; i.e., there is no evidence for Ga-Ga or Sb-Sb bonds in either the zinc blende or the diamond structure. However, the critical composition x_c was found to depend upon the film growth conditions and a model is presented which explains this result on the basis of morphological effects on film growth kinetics.

PACS numbers: 61.10.-i, 61.55.Hg

Epitaxial metastable $(\text{III-V})_{1-x}(\text{IV}_2)_x$ alloys,¹ including $(\text{GaAs})_{1-x}(\text{Si}_2)_x$,² $(\text{GaAs})_{1-x}(\text{Ge}_2)_x$,³ $(\text{GaSb})_{1-x}(\text{Ge}_2)_x$,⁴ and, more recently, $(\text{GaSb})_{1-x}(\text{Sn}_2)_x$,⁵ have been grown by sputter deposition onto (100) GaAs. In the case of $(\text{GaAs})_{1-x}(\text{Ge}_2)_x$, which has also been grown by pyrolytic decomposition from the vapor phase,⁶ and $(\text{GaSb})_{1-x}(\text{Ge}_2)_x$, alloys have been obtained with compositions spanning the pseudobinary phase diagram. Measurements^{3,7} of the direct Γ -point band gap E_0 as a function of composition x showed very large and nonparabolic bowing. Newman and co-workers^{7,8} proposed a model, which includes a second-order phase transition from a zinc blende to a diamond structure at the position of maximum bowing, to explain the results. However, Holloway and Davis⁹ have recently described the experimental results with a model which assumes perfect short-range order and in which the bowing is not dependent upon the existence of a long-range order-disorder transition. Perfect short-range order in this context implies no Ga-Ga or As-As nearest-neighbor pairs.

The fact that both models provide reasonable fits to the data while starting from very different assumptions concerning the atomic arrangement of the alloys is due to the fact that the energy gap, an optoelectronic property, is related to the atomic structure in an indirect manner. It is not surprising that the structure cannot be uniquely determined from a measurement of E_0 vs x . In this paper we present the initial results of an experimental investigation of the structure of metastable $(\text{III-V})_{1-x}(\text{IV}_2)_x$ alloys. The extended x-ray-absorption fine-structure (EXAFS) technique was used to determine short-range order while x-ray diffraction was used to determine long-range order.

In the case of $(\text{GaAs})_{1-x}(\text{Ge}_2)_x$, the atomic numbers of the constituent species are so close that it is experimentally difficult to distinguish among back-

scattering EXAFS signals from Ga, As, and Ge. Thus, the present experiments were carried out on an analogous alloy system which also exhibits a large and nonparabolic bowing in E_0 vs x ,¹⁰ $(\text{GaSb})_{1-x}(\text{Ge}_2)_x$. Direct experimental determination of both long-range and short-range order can be carried out in these alloys since the atomic number of Sb is sufficiently far separated from Ga and Ge that Sb can be easily distinguished.

The $(\text{GaSb})_{1-x}(\text{Ge}_2)_x$ films were grown in a multi-target rf sputtering system which has been described in detail elsewhere.⁴ Polycrystalline GaSb and single-crystal Ge wafers, both with purities better than 99.999%, were used as targets. The system base pressure was $\sim 10^{-7}$ Torr, and sputtering was carried out in gettered Ar at a pressure of 15 mTorr. The induced negative potential on the substrate with respect to the positive space-charge region in the discharge was 75 V. Corning No. 00 glass slides, $\sim 75 \mu\text{m}$ thick, were used as substrates. The films were $\sim 4 \mu\text{m}$ thick, grown at a rate of $1.0 \mu\text{m h}^{-1}$, and were deposited on both sides of each substrate. The growth temperature ranged from 325 °C to 375 °C, but in all cases it was low enough that an excess Sb partial pressure was not required.

Film compositions were determined by wavelength dispersive analysis in a JEOL electron microprobe with use of elemental and compound reference standards. Matrix corrections were carried out by use of an on-board computer. The reported film compositions $-x = 0, 0.25, 0.29, 0.38, 0.46, 0.58, \text{ and } 1.0$ —are accurate to ± 0.5 at.% and are in good agreement with Ge concentrations determined by EXAFS from a comparison of the Ga and Ge K -edge steps. The EXAFS measurements were carried out in the standard absorption mode¹¹ on beamline IV-1 at the Standard Synchrotron Radiation Laboratory. The K edges of Ga

and Ge were measured at 50 K for all x , allowing effects due to a thermal Debye-Waller factor to be ignored.

The x-ray-absorption data were analyzed in the usual manner.¹² A linear fit to the data below the edge was subtracted in order to isolate the K edge. The oscillatory portion of the K edge was further isolated by subtracting a spline and normalized by dividing by the K -edge step to give $\chi(E)$. The photon energy E , in electronvolts, was converted to photoelectron wave number k expressed in inverse angstroms by use of the relation $k = [0.263(E - E_0)]^{1/2}$, where E_0 is chosen to be at the midpoint of the edge. Figure 1 shows the resulting $\chi(k)$ for $x = 0.25$ and illustrates the quality of the data.

The $\chi(k)$ data were Fourier filtered to isolate the first-coordination-shell contribution.¹² The pure GaSb and Ge data were used as standards to determine the contributions from various center atoms and backscattering-atom pairs in the alloys. Ga-Sb and Ge-Ge pairs were determined directly, while Ga-Ga, Ge-Ga, and Ge-Sb were calculated from the directly determined results by using theory¹³ to obtain the central-atom and backscattering-atom changes between Ge and Ga. Since these changes involve a $\Delta Z = 1$, they are small and should therefore be accurately determined. The first-shell data of the alloys were then fitted by a superposition of the appropriate standards, with coordination numbers, interatomic distances, and disorder allowed to be either independent or dependent parameters.

The best fit to the EXAFS data gave the number of Sb nearest-neighbor atoms N_{Sb} shown in Fig. 2. The triangles correspond to Ga centers and the circles to Ge centers. The Ga-Sb, Ge-Sb, and Ga-Ge distances were found to be 2.65 ± 0.02 , 2.67 ± 0.04 , and 2.46 ± 0.03 Å, respectively. The total coordination number about the Ga atoms was 3.9 ± 0.2 , while that

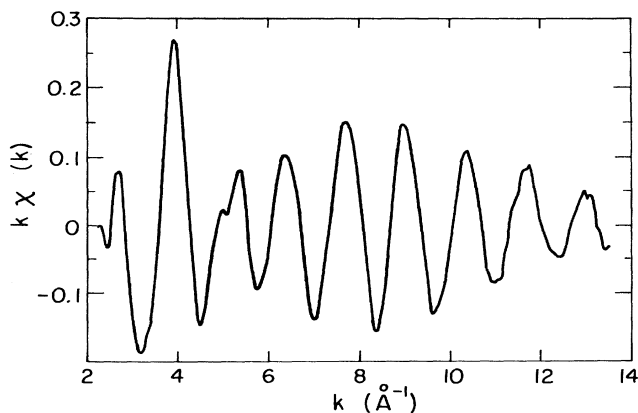


FIG. 1. EXAFS data $k\chi(k)$ about a Ga center atom for $x = 0.25$ taken at 50 K.

about the Ge atoms was 3.6 ± 0.2 . The number of Sb neighbors N_{Sb} was determined to about ± 0.1 . N_{Sb} , being quite insensitive to the other parameters assumed in the fit, was determined to the greatest accuracy. The results obtained were found to be independent of whether the mean square disorder σ^2 was varied or set equal to zero. In the cases in which it was varied it was found to be always quite small (≤ 0.001 Å²).

For comparison, N_{Sb} expected for alloys with perfect and random short-range order are plotted as solid lines in Fig. 2. In the perfect short-range order case, and with the assumption that the Ge is equally distributed among the Ga and Sb sites, the average number of Sb nearest neighbors to a Ga atom is

$$N_{Sb} = 4(1 - x), \quad (1)$$

while for random short-range order,

$$N_{Sb} = 2(1 - x). \quad (2)$$

For the Ge center, N_{Sb} is given by Eq. (2), with the assumption that the Ge is randomly distributed among the Ga and Sb sites.

The first observation to make from the data in Fig. 2 is that the number of Sb atoms around the Ga center falls along the line representing perfect short-range order. This indicates that any phase transition that may occur as a function of x in these samples does not alter the short-range order. The results for Ge as a center atom are not fitted by Eq. (2), clearly indicating that the Ge is not randomly distributed throughout the volume of the sample.

A model which can explain the smaller value of Sb

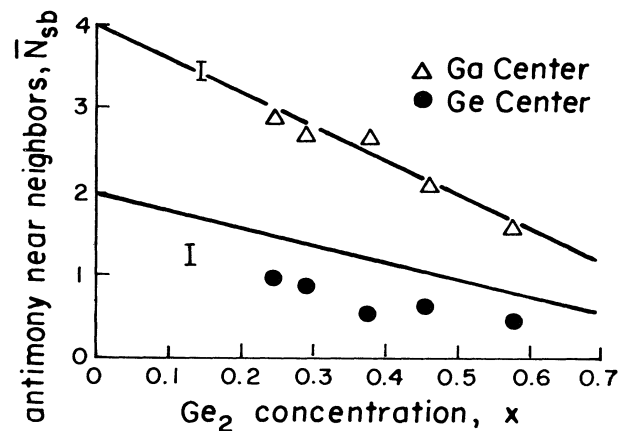


FIG. 2. Number of antimony neighbors N_{Sb} about Ga (triangles) and Ge (circles) center atoms. The upper solid line is the expected result for Ga with perfect short-range order, while the lower solid line is for complete random order. The experimental errors in the points are indicated by the error bars.

atoms and total coordination about the Ge atoms is one in which the Ge in the grain boundaries preferentially substitutes in Sb sites at dislocations and other defect sites where the average coordination number is decreased. Since the Ge atom is smaller than the Sb atom such a substitution would lower the strain energy. The EXAFS results require about 30% of the Ge atoms to be in the grain boundary defects. Such a grain boundary volume in these films with grain sizes of the order of 1000 Å is not unreasonable. Within the grains, the Ge atoms substitute for the Ga and Sb sites with equal probability and thus are randomly distributed.

A feature that is clear from Fig. 1 is that the short-range order is as perfect as it can be. In particular, there is no evidence that a zinc-blende-to-diamond transition is affecting the short-range order. The Newman-Dow (ND) model, which presupposes a change in long-range order at some critical composition, also assumes a corresponding change in short-range order. However, the latter is due to mathematical simplifications in the theory and is not an inherent requirement. The Holloway-Davis (HD) model assumption of perfect short-range order is in agreement with our results. However, this does not mean that the HD model is correct and the ND assumption of a zinc-blende-to-diamond transition is in error, as we show below.

The alloys were also analyzed by x-ray diffractometry of both solid and pulverized powder samples. All films were found to exhibit a (220) preferred orientation, as has been reported previously⁴ for $(\text{GaSb})_{1-x}(\text{Ge}_2)_x$ films grown on amorphous substrates. In order to test for the occurrence of a zinc-blende-to-diamond transition, the intensity ratio r_1 of superlattice to fundamental reflections was determined for each sample normalized to pure GaSb. The (420)/(331) intensity ratio was used for diffraction from the films since the Bragg angles corresponding to these peaks are fairly close, thus minimizing corrections for nonsymmetric ω -drive settings. In the case of the powder samples, the (200)/(400) intensity ratio was used.

The ratio r_1 , which is a measure¹⁴ of the long-range order parameter S , was found to be above the detection limits of both measurements only for a sample with $x=0.1$ (not used in the EXAFS measurements). The r_1 value was 0.19 ± 0.06 for (420)/(331) and 0.10 ± 0.02 for (200)/(400). This result is quite different from the behavior found for single-crystal $(\text{GaSb})_{1-x}(\text{Ge}_2)_x$ films grown on (100) GaAs, where $r_1\{(200)/(400)\}$ persisted to $x \approx 0.3$.¹⁵ The low value of $r_1=0.10$, corresponding to the present $x=0.1$ sample, did not occur until $x \approx 0.27$ in the epitaxial films. Thus, the polycrystalline films grown on amorphous substrates exhibited a more rapid decrease in $S(x)$ than the single-crystal films grown on (100) GaAs.

The above results indicate that $S(x)$ in these metastable alloys depends upon the experimental growth conditions. This is perhaps not surprising since the alloys are, after all, not in thermal equilibrium. A simple model of film formation can explain the observed variation in $S(x)$.

The model assumes the perfect short-range order found experimentally, namely, that there are no Ga-Ga or Sb-Sb nearest-neighbor bonds, and that Ge has an equal probability of being a nearest neighbor with either Ga or Sb. The alloy is formed by individual atoms of Ga, Sb, and Ge filling nearest-neighbor sites to an already occupied site in a face-centered-cubic lattice with a two-atom basis. The only variable is the morphology of film growth: i.e., whether growth proceeds spherically around a point (three-dimensional nucleation) or epitaxially by layer growth (two-dimensional nucleation). A computer simulation of film growth was carried out as a function of x for these two cases.

In the two-dimensional nucleation case, a (100) zinc-blende surface was used as the substrate template in the computer simulation just as in the actual experiment. Perfect short-range order was maintained, even across the film-substrate interface. Thus, Sb-As nearest neighbors were also prohibited. The film area was varied in the simulation from 70×70 to 100×100 cubic lattice constants without any significant differences in the results. Long-range order was found to persist up to $x \approx 0.3$ and to vanish for higher concentrations, in good agreement with experimental results. For the three-dimensional nucleation case, $x_c < 0.18$.

In summary, experimental results were presented to show that a zinc-blende-to-diamond transition is not a thermodynamic but a kinetic one governed by the perfect short-range order and the morphology of growth. The composition x_c at which the transition takes place depends upon the film growth conditions, varying from ~ 0.1 for polycrystalline films nucleated three dimensionally on amorphous substrates to ~ 0.3 for epitaxial growth on (100) GeAs surfaces. Nevertheless, the EXAFS results showed that the short-range order was perfectly maintained for all samples investigated out to $x=0.58$, well beyond the region of long-range zinc-blende order. These results suggest the exciting possibility of being able to tailor the long-range order in these alloys through the choice of film growth conditions and substrate.

The authors are indebted to Professor R. Besserman of the Technion Institute for suggesting the experiments reported here. The research was supported in part by the National Science Foundation through Grants No. PCM82-04234 and No. DMR80-22221 and in part by the Materials Science Division of the U. S. Department of Energy under Contract No. DE-AC02-76ER01198. We also acknowledge the use of the facilities at the Center for Microanalysis at the University

of Illinois, which is partially supported by the U. S. Department of Energy. The work reported herein was partially done at Stanford Synchrotron Radiation Laboratory which is supported by the U. S. Department of Energy Office of Basic Energy Science and by the National Institutes of Health, Biotechnology Resource, Division of Research Resources.

^(a)New address: Department of Physics, Wesleyan University, Middletown, Conn. 06457.

¹J. E. Greene, *J. Vac. Sci. Technol.* **1**, 229 (1983).

²A. J. Noreika and M. H. Francombe, *J. Appl. Phys.* **45**, 3690 (1974).

³S. A. Barnett, M. A. Ray, A. Lastras, B. Kramer, J. E. Greene, and P. M. Raccach, *Electron. Lett.* **18**, 891 (1982).

⁴K. C. Cadien, A. H. Eltoukhy, and J. E. Greene, *Appl. Phys. Lett.* **38**, 773 (1981), and *Vacuum* **31**, 253 (1981).

⁵L. Romano, S. A. Barnett, and J. E. Greene, unpublished.

⁶Zh. I. Alferov, M. Z. Zhingarev, S. G. Konnikov, I. I. Mogan, V. P. Ulin, V. E. Umanski, and B. S. Yavich, *Fiz. Tekh. Poluprovodn.* **16**, 831 (1982) [*Sov. Phys. Semicond.* **16**, 532 (1982)].

⁷K. E. Newman, A. Lastras-Martinez, B. Kramer, S. A. Barnett, M. A. Ray, J. D. Dow, J. E. Greene, and P. M. Raccach, *Phys. Rev. Lett.* **50**, 1466 (1983).

⁸K. E. Newman and J. D. Dow, *Phys. Rev. B* **27**, 7495 (1983).

⁹H. Holloway and L. C. Davis, *Phys. Rev. Lett.* **53**, 830 (1984).

¹⁰S. I. Shah, B. Kramer, P. M. Raccach, D. Aspnes, and J. E. Greene, unpublished.

¹¹See, e.g., E. A. Stern and S. M. Heald, in *Handbook on Synchrotron Radiation*, edited by E. E. Koch (North-Holland, New York, 1983), Vol. 1, pp. 955–1014.

¹²E. A. Stern, D. E. Sayers, and F. W. Lytle, *Phys. Rev. B* **11**, 4836 (1975).

¹³B. K. Teo and P. A. Lee, *J. Am. Chem. Soc.* **101**, 2815 (1979).

¹⁴B. E. Warren, *X-Ray Diffraction* (Addison-Wesley, Reading, Mass., 1969), Chap. 12.

¹⁵S. I. Shah, B. Kramer, and J. E. Greene, unpublished.